

Are Debris Disks and Massive Planets Correlated?

M. Silverstone – University of Arizona
et al.

Deposited 06/13/2019

Citation of published version:

Moro-Martín, A., et al. (2007): Are Debris Disks and Massive Planets Correlated? *The Astronomical Journal*, 658(2). DOI: <https://doi.org/10.1086/511746>

ARE DEBRIS DISKS AND MASSIVE PLANETS CORRELATED?

AMAYA MORO-MARTÍN,¹ JOHN M. CARPENTER,² MICHAEL R. MEYER,³ LYNNE A. HILLENBRAND,² RENU MALHOTRA,⁴
 DAVID HOLLENBACH,⁵ JOAN NAJITA,⁶ THOMAS HENNING,⁷ JINYOUNG S. KIM,³ JEROEN BOUWMAN,⁷
 MURRAY D. SILVERSTONE,³ DEAN C. HINES,⁸ SEBASTIAN WOLF,⁷ ILARIA PASCUCCI,³
 ERIC E. MAMAJEK,⁹ AND JONATHAN LUNINE⁴

Received 2006 November 2; accepted 2006 December 8

ABSTRACT

Using data from the *Spitzer Space Telescope* Legacy Science Program Formation and Evolution of Planetary Systems (FEPS), we have searched for debris disks around nine FGK stars (2–10 Gyr), known from radial velocity (RV) studies to have one or more massive planets. Only one of the sources, HD 38529, has excess emission above the stellar photosphere; at 70 μm the signal-to-noise ratio in the excess is 4.7, while at $\lambda < 30 \mu\text{m}$ there is no evidence of excess. The remaining sources show no excesses at any *Spitzer* wavelengths. Applying survival tests to the FEPS sample and the results for the FGK survey recently published in Bryden et al., we do not find a significant correlation between the frequency and properties of debris disks and the presence of close-in planets. We discuss possible reasons for the lack of a correlation.

Subject headings: circumstellar matter — Kuiper Belt — infrared: stars — planetary systems —
 stars: individual (HD 6434, HD 38529, HD 80606, HD 92788, HD 106252, HD 121504,
 HD 141937, HD 150706, HD 179949, HD 190228)

1. INTRODUCTION

During the last two decades, space-based infrared observations, first with the *Infrared Astronomical Satellite (IRAS)* and then with the *Infrared Space Observatory (ISO)* and *Spitzer*, have shown that many main-sequence stars are surrounded by dust disks (namely, debris disks). These disks are generally observed by their infrared emission in excess over the stellar photosphere, but in some cases the disks have been spatially resolved and extend to hundreds of AU from the central star. Dust particles are affected by radiation pressure, Poynting-Robertson and stellar wind drag, mutual collisions, and collisions with interstellar grains, and all these processes contribute to make the lifetime of the dust particles significantly shorter than the age of the star-disk system. It is therefore thought that this dust is being replenished by a reservoir of undetected dust-producing planetesimals (Backman & Paresce 1993), like the asteroids, Kuiper Belt objects (KBOs), and comets in our solar system. This represented a major leap in the search for other planetary systems; by 1983, a decade before extrasolar planets were discovered, *IRAS* observations proved that there is planetary material surrounding nearby stars (Aumann et al. 1984).

Preliminary results from *Spitzer* observations of FGK (solar type) stars indicate that the frequency of 24 μm excesses (tracing warm dust at asteroid belt-like distances) decreases from $\sim 30\%$ – 40% for ages < 50 Myr to $\sim 9\%$ for 100 Myr–200 Myr and to $\sim 1.2\%$ for ages > 1 Gyr (Siegler et al. 2007; Gorlova et al. 2006;

Stauffer et al. 2005; Beichman et al. 2005; Kim et al. 2005; Bryden et al. 2006). On the other hand, Bryden et al. (2006) estimated that the excess rate at 70 μm (tracing colder dust at Kuiper Belt-like distances) is $13\% \pm 5\%$ and is not correlated with stellar age on Gyr timescales. It is also found that FGK stars show large variations in the amount of excess emission at a given stellar age and that the upper envelope of the ratio of excess emission to the stellar photosphere at 24 μm decays as $1/t$ for ages > 20 Myr (Siegler et al. 2007).

These observations are consistent with numerical simulations of the evolution of dust generated from the collision of planetesimals around solar-type stars (Kenyon & Bromley 2005). These models predict that after 1 Myr there is a steady $1/t$ decline of the 24 μm excess emission, as the dust-producing planetesimals become depleted. It is also found that this decay is punctuated by large spikes produced by individual collisional events between planetesimals 100–1000 km in size. These events initiate a collisional cascade leading to short-term increases in the density of small grains, which can increase the brightness density of the disk by an order of magnitude, in broad agreement with the high degree of debris disk variability observed by *Spitzer* (Rieke et al. 2005; Siegler et al. 2007).

However, these models do not include the presence of massive planets, and the study of the evolution of the solar system indicates that they may strongly affect the evolution of debris disk. There has been one major event in the early solar system evolution that likely produced large quantities of dust. Between 4.5 and 3.85 Gyr ago there was a heavy cratering phase that resurfaced the Moon and the terrestrial planets, creating the lunar basins and leaving numerous impact craters on the Moon, Mercury, and Mars. This Heavy Bombardment ended abruptly ~ 3.85 Gyr ago, and since then the impact flux has been at least an order of magnitude smaller. During the last 20–200 Myr of the Heavy Bombardment epoch, a period known as the Late Heavy Bombardment (LHB), there was increased cratering activity, which came after a relatively calm period of several hundred million years and could have been created by a sudden injection of impact objects from the main asteroid belt into the terrestrial zone.

¹ Department of Astrophysical Sciences, Princeton University, Princeton, NJ 08544; amaya@astro.princeton.edu;

² Department of Astronomy, California Institute of Technology, Pasadena, CA 91125.

³ Steward Observatory, University of Arizona, Tucson, AZ 85721.

⁴ Department of Planetary Sciences, University of Arizona, Tucson, AZ 85721.

⁵ NASA Ames, Moffet Field, CA 04035.

⁶ National Optical Astronomy Observatory, Tucson AZ 85721.

⁷ Max-Planck-Institut für Astronomie, Heidelberg, Germany.

⁸ Space Science Institute, Boulder, CO 80301.

⁹ Harvard-Smithsonian Center for Astrophysics, Cambridge, MA 02138.

TABLE 1
STELLAR PROPERTIES

Source (HD No.)	Spectral Type	Distance ^a (pc)	Age (Gyr)	T_{eff} (K)	$\log L$ ($\log L_{\odot}$)	M (M_{\odot})	[Fe/H]
6434.....	G2/3 V ^b	40 ± 1	12 ± 1 ^c	5835 ^d	0.05 ± 0.02 ^e	0.84 ± 0.05 ^f	−0.52 ^d
38529.....	G8 III–G IV ^b	42 ± 2	3.5 ± 1 ^g	5697 ^h	0.80 ^h	1.47 ^h	0.445 ^h
80606.....	G5 ⁱ	58 ± 20	6 ^j	5573 ^h	−0.15 ^h	1.06 ^h	0.343 ^h
92788.....	G6 V ^k	32 ± 1	6 ± 2 ^l	5836 ^h	0.01 ^h	1.13 ^h	0.318 ^h
106252.....	G0 ⁱ	37 ± 1	5.5 ± 1 ^m	5870 ^h	0.11 ^h	1.01 ^h	−0.07 ^h
121504.....	G2 V ⁿ	44 ± 2	2 ± 1 ^o	6075 ^d	0.19 ± 0.04 ^e	1.03 ± 0.06 ^f	0.16 ^d
141937.....	G2/3 V ^p	33 ± 1	2.6 ± 1 ^q	5847 ^h	0.07 ^h	1.08 ^h	0.129 ^h
179949.....	F8 V ^p	27 ± 1	2.5 ± 1 ^r	6168 ^h	0.27 ^h	1.21 ^h	0.137 ^h
190228.....	G5 IV ^s	62 ± 3	5 ^r	5348 ^h	0.63 ^h	1.21 ^h	−0.180 ^h

^a *Hipparcos* Catalog (Perryman et al. 1997).^b Houk (1980).^c Barbieri & Gratton (2002); Nordstrom et al. (2004); Ibukiyama & Arimoto (2002).^d Santos et al. (2004).^e Computed from FEPS database.^f Nordstrom et al. (2004).^g Valenti & Fischer (2005); Gonzalez et al. (2001).^h Valenti & Fischer (2005).ⁱ Cannon & Pickering (1918–1924).^j E. E. Mamajek (2007, in preparation).^k Houk & Swift (1999).^l Wright et al. (2004); Laws et al. (2003); Gonzalez et al. (2001).^m Valenti & Fischer (2005); Wright et al. (2004); Laws et al. (2003); E. E. Mamajek (2007, in preparation).ⁿ Houk & Cowley (1975).^o Barbieri & Gratton (2002); E. E. Mamajek (2007, in preparation).^p Houk & Smith-Moore (1988).^q Barbieri & Gratton (2002); Nordstrom et al. (2004); Laws et al. (2003); Valenti & Fischer (2005); E. E. Mamajek (2007, in preparation).^r Nordstrom et al. (2004); Valenti & Fischer (2005).^s Jaschek (1978).

The orbits of these objects became unstable, likely due to the orbital migration of the giant planets, which caused a resonance sweeping of the asteroid belt and a large-scale ejection of asteroids into planet-crossing orbits (Strom et al. 2005; Gomes et al. 2005). This event, triggered by the migration of the giant planets, would have been accompanied by a high rate of asteroid collisions, and the corresponding high rate of dust production would have caused a large spike in the warm dust luminosity of the solar system. Similarly, a massive clearing of planetesimals is thought to have occurred in the Kuiper Belt (KB). This is inferred from estimates of the total mass in the KB region, 30–55 AU, ranging from $0.02 M_{\oplus}$ (Bernstein et al. 2004) to $\sim 0.08 M_{\oplus}$ (Luu & Jewitt 2002), insufficient to form the KBOs within the age of the solar system (Stern 1996). It is estimated that the primordial KB had a mass of 30–50 M_{\oplus} between 30 and 55 AU and was heavily depleted after Neptune formed and started to migrate outward (Malhotra et al. 2000; Levison et al. 2007). This resulted in the clearing of KBOs with perihelion distances near or inside the present orbit of Neptune and in the excitation of the KBO orbits. The latter increased the relative velocities of KBOs from 10 m s^{-1} to $>1 \text{ km s}^{-1}$, making their collisions violent enough to grind down a significant mass of the KBOs to dust and blow it away by radiation pressure.

The evolution of debris disks may therefore be strongly affected by the presence of planets; in its early history, a star with planetary companions may be surrounded by a massive debris disk while the planets are undergoing orbital migration, whereas at a later stage, the star would harbor a sparse dust disk after the dynamical rearrangement of the planets is complete (Meyer et al. 2007); at very late stages, 2–10 Gyr, the production of dust may undergo occasional bursts due to major collisions of planetesimals stirred up by the planets. In addition to their effect on the dust production rates, massive planets can also affect the dynamics of

the dust grains. Examples include the trapping of dust particles in mean motion resonances and their ejection due to gravitational scattering (Liou & Zook 1999; Moro-Martín & Malhotra 2002, 2005).

In this paper, we search for debris disks around nine stars known from RV studies to harbor one or more massive planets. These stars are drawn from the *Spitzer* Legacy program Formation and Evolution of Planetary Systems (FEPS). The properties of the stars and their planetary companions can be found in Tables 1 and 2. The observations and data reduction are briefly described in § 2, and the resulting spectral energy distributions (SEDs) are presented in § 3. In § 4 we explore the correlation of the frequency of dust emission with the presence of known planets by applying survival tests to the FEPS sample and the FGK star survey published in Bryden et al. (2006). Finally, § 5 discusses the interpretation of our results. HD 38529, the only planet star in the FEPS sample with an excess emission, is discussed in detail in Moro-Martín et al. (2007).

2. OBSERVATIONS AND DATA REDUCTION

An overview of the FEPS program is given in Meyer et al. (2004, 2006), and a detailed description of the data acquisition and data reduction is given in Hines et al. (2005) and J. M. Carpenter et al. (2007, in preparation). The Multiband Imaging Photometer for *Spitzer* (MIPS; Rieke et al. 2004) was used to obtain observations at 24 and 70 μm using the small-field photometry mode with 2–10 cycles of 3 and 10 s integration times, respectively. The data were first processed by the *Spitzer* Science Center (SSC) pipeline version S13, and further processing was done by the FEPS team, the details of which can be found in J. M. Carpenter et al. (2007, in preparation).

At 24 μm , point-spread function (PSF) fitting photometry was performed using the APEX module in MOPEX (Makovoz

TABLE 2
ORBITAL CHARACTERISTICS OF KNOWN PLANETARY COMPANIONS

Planet (HD No.)	$M_p \sin i$ (M_J)	Period (days)	a_p (AU)	e_p	N_{obs}	Reference
6434b.....	0.397(59)	21.9980(90)	0.1421(82)	0.170(30)	130	1
38529b.....	0.852(74)	14.3093(13)	0.1313(76)	0.248(23)	162	2
38529c.....	13.2(1.1)	2165(14)	3.72(22)	0.3506(85)	162	2
80606b.....	4.31(35)	111.4487(32)	0.468(27)	0.9349(23)	46	2
	3.90(9)	111.81(23)	0.47	0.9227(12)	61	3
92788b.....	3.67(30)	325.81(26)	0.965(56)	0.334(11)	58	2
	3.58	325.0(5)	0.96	0.35(1)	55	1
106252b.....	7.10(65)	1516(26)	2.60(15)	0.586(65)	15	2
	7.56	1600(18)	2.7	0.471(28)	40	4
121504b.....	1.22(17)	63.330(30)	0.329(19)	0.030(10)	100	1
141937b.....	9.8(1.4)	653.2(1.2)	1.525(88)	0.410(10)	81	5
179949b.....	0.916(76)	3.092514(32)	0.0443(26)	0.022(15)	88	2
190228b.....	4.49	1146(16)	2.25	0.499(30)	51	4

NOTES.—HD 38529 has two known planets. The multiple entries for the other stars correspond to different estimates for the same planet, a_p and e_p are the semimajor axis and eccentricity of the planet, and N_{obs} is the number of RV observations. The number in parentheses indicates the uncertainty in the last significant figures.

REFERENCES.—(1) Mayor et al. 2004; (2) Butler et al. 2006; (3) Naef et al. 2001; (4) Perrier et al. 2003; (5) Udry et al. 2002.

& Marleau 2005) with a fitting radius of 21 pixels on the individual Basic Calibrated Data (BCD) images. Fluxes were computed by integrating the PSF to a radius of 3 pixels and then applying an aperture correction of 1.600 to place the photometry on the same scale as described in the MIPS Data Handbook. The S13 images were processed using a calibration factor of $0.0447 \text{ MJy sr}^{-1}$. We adopt a calibration uncertainty of 4%, as stated on the SSC MIPS Web pages.

The raw MIPS $70 \mu\text{m}$ images were processed with the SSC pipeline version S13. The individual BCD images were formed into mosaics with $4''$ pixel sizes using the Germanium Reprocessing Tools (GeRT) software package S14.0 version 1.1 developed by the SSC. The GeRT package performs column filtering on the BCD images to remove streaks in the BCD images and then performs a time median filter to remove residual pixel response variations. A $40'' \times 40''$ region centered on the source position was masked when computing the time and column filtering such that the filtering process is not biased by the source. The filtered images were formed into mosaics using MOPEX. Aperture photometry was performed on the MIPS $70 \mu\text{m}$ mosaics using a custom modified version of IDLPHOT. The adopted aperture radius of $16''$ was chosen to optimize the signal to noise ratio (S/N) for faint sources. The sky level was computed as the mean value of the pixels in a sky annulus that extends from $40''$ to $60''$. The photometry uncertainty is given by $\sigma = \Omega \sigma_{\text{sky}} (N_{\text{ap}})^{1/2} \eta_{\text{sky}} \eta_{\text{corr}} (1.0 + N_{\text{ap}}/N_{\text{sky}})^{1/2}$, where σ_{sky} is the standard deviation in the sky annulus surface brightness, Ω is the pixel solid angle, N_{sky} and N_{ap} are the number of pixels in the sky annulus and in the aperture, and η_{sky} and η_{corr} are correction factors that account for the presence on the mosaic of nonuniform noise and of correlated noise, respectively. We used $\eta_{\text{sky}} = 2.5$ and $\eta_{\text{corr}} = 1.40$ (see the full description in J. M. Carpenter et al. 2007, in preparation). The adopted calibration factor is $702 \text{ MJy sr}^{-1} (\text{DN s}^{-1})^{-1}$, with an uncertainty of 7%, as described on the SSC MIPS Web pages.

The Infrared Spectrograph (IRS; Houck et al. 2004) was used to obtain low-resolution ($R = 70\text{--}120$) spectra from 7.4 to $38 \mu\text{m}$, with integration times per exposure of 6 and 14 s for the Short-Low ($7.4\text{--}14.5 \mu\text{m}$) and Long-Low ($14.0\text{--}38.0 \mu\text{m}$), respectively. The data were initially processed with the SSC pipeline S10.5.0, with further processing described in J. Bouwnman et al. (2007, in preparation). From the spectra, synthetic photometric points

were calculated at $13 \mu\text{m}$ with a rectangular bandpass between 12.4 and $14.0 \mu\text{m}$, at $24 \mu\text{m}$ with the same bandpass shape as the MIPS 24 filter, and at $33 \mu\text{m}$ with a rectangular bandpass between 30 and $35 \mu\text{m}$. The estimated calibration uncertainty in the synthetic photometric is 6% (J. M. Carpenter et al. 2007, in preparation). The spectra are generally not reliable beyond $35 \mu\text{m}$, although we found that for HD 6434, HD 121504, and HD 80606 it is very noisy beyond 34 , 33 , and $30 \mu\text{m}$, respectively, making the $33 \mu\text{m}$ photometric points unreliable for the last two sources. The latter is flagged by the SSC as nonnominal, possibly due to a failure in the peak-up.

The Infrared Array Camera (IRAC; Fazio et al. 2004) was used to obtain observations at 3.6 , 4.5 , and $8.0 \mu\text{m}$ in subarray mode. Initial processing of the data was done with the SSC pipeline S13, with further processing as described in J. M. Carpenter et al. (2007, in preparation). Aperture photometry on individual IRAC frames was performed using a custom modified version of IDLPHOT using an aperture radius of 3 pixels ($1 \text{ pixel} \sim 1.2''$), with the background annulus extending from 10 to 20 pixels centered on the star. The internal uncertainty was estimated as the standard deviation of the mean of the photometry measured at the four dither positions. We adopted calibration factors of 0.1088 , 0.1388 , and $0.2021 \text{ MJy sr}^{-1} (\text{DN s}^{-1})^{-1}$ for IRAC 3.6 , 4.5 , and $8 \mu\text{m}$, respectively, and calibration uncertainties of 2% (Reach et al. 2005).

3. SPECTRAL ENERGY DISTRIBUTIONS AND EXCESS EMISSION

The SEDs are shown in Figure 1 and include the *Spitzer* photometric measurements, observations made by *IRAS*, *Tycho*, and *2MASS* and, in some cases, upper limits at 1.2 mm from Carpenter et al. (2005). For each star, the results from the *Spitzer* photometric measurements and their internal uncertainties are listed in the first entry of Table 3 (in rows indicated by “obs”). The reported fluxes arise from both the photosphere of the star and the thermal emission of the dust (if present). For all targets, observations are sufficient to detect the photosphere of the star at all *Spitzer* wavelengths $< 33 \mu\text{m}$, making it possible to detect small dust excesses (limited mainly by the calibration uncertainties). To estimate the contribution from the dust alone, we need to subtract the photospheric emission, given in the second entry of Table 3 (in rows indicated by “model”). The Kurucz model calculations are described

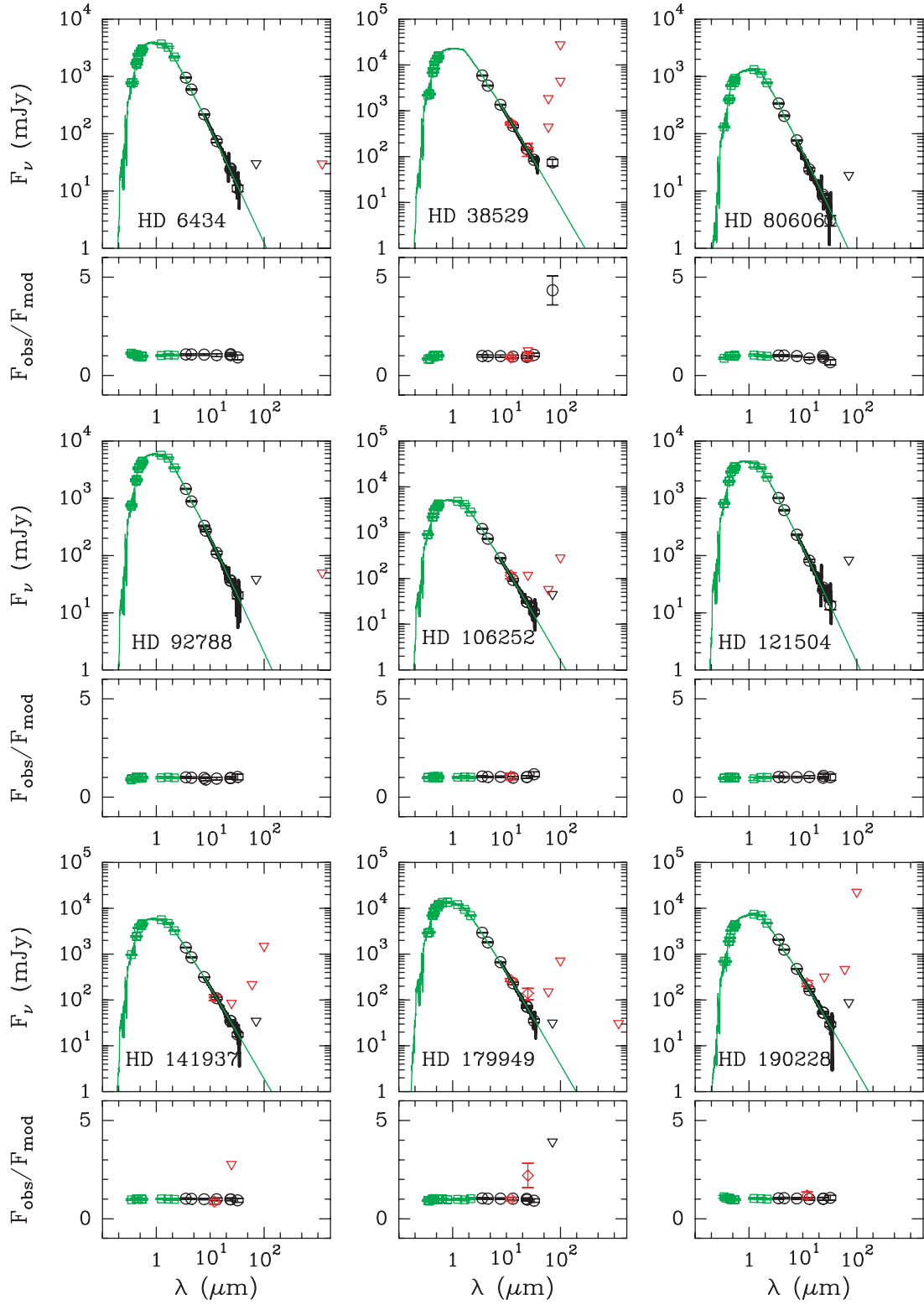


FIG. 1.— Spectral energy distributions (SEDs) of the nine planet-bearing stars in the FEPS program. The green line represents the Kurucz model. The black thicker line represents the IRS low-resolution spectrum. The photometric points are identified as follows: green squares represent ground-based observations (including Tycho and 2MASS); black circles represent *Spitzer* observations (IRAC, MIPS, and synthetic photometry from IRS); red diamonds represent *IRAS* observations. In all cases, the error bars correspond to 1σ uncertainties. Upper limits are represented by triangles and are given when $F/\Delta F < 3$ and placed at $F + 3\Delta F$ if $F > 0$ or $3\Delta F$ if $F < 0$. Black triangles show the upper limits for *Spitzer* 70 μm , and red triangles show those for *IRAS* and 1.2 mm.

TABLE 3
Spitzer PHOTOMETRY AND KURUCZ STELLAR MODELS FOR FEPS TARGETS WITH PLANETS

Source (HD No.)		IRAC 3.6 (μm)	IRAC 4.5 (μm)	IRAC 8 (μm)	IRS 13 (μm)	MIPS 24 (μm)	IRS 24 (μm)	IRS 33 (μm)	MIPS 70 (μm)	S/N _{exc} at 70 μm	1200 (μm)
6434.....	obs	952 \pm 7	603 \pm 7	215 \pm 1	74.9 \pm 0.8	23.9 \pm 0.2	25.0 \pm 0.8	11 \pm 1	8.0 \pm 7.4	0.7	0 \pm 10
	model	892 \pm 28	565 \pm 17	203 \pm 6	73 \pm 2	23.2 \pm 0.7	23.2 \pm 0.7	12.2 \pm 0.4	2.6 \pm 0.1
38529.....	obs	5893 \pm 42	3634 \pm 44	1340 \pm 9	467 \pm 5	150 \pm 1	146 \pm 2	86 \pm 2	75 \pm 11	4.7	...
	model	5935 \pm 283	3689 \pm 168	1360 \pm 66	487 \pm 24	156 \pm 8	156 \pm 8	82 \pm 4	17.4 \pm 0.8
80606.....	obs	340 \pm 2	210 \pm 3	75.5 \pm 0.5	23.8 \pm 0.7	8.65 \pm 0.08	7.9 \pm 0.3	3.1 \pm 0.6	3 \pm 5	0.5	...
	model	335 \pm 12	208 \pm 7	77 \pm 3	27 \pm 1	8.8 \pm 0.3	8.8 \pm 0.3	4.6 \pm 0.2	0.98 \pm 0.04
92788.....	obs	1447 \pm 10	891 \pm 11	323 \pm 2	111 \pm 1	36.1 \pm 0.3	37 \pm 1	20 \pm 2	11 \pm 9	0.8	5 \pm 15
	model	1438 \pm 52	902 \pm 31	329 \pm 12	118 \pm 4	38 \pm 1	38 \pm 1	19.8 \pm 0.7	4.2 \pm 0.2
106252.....	obs	1200 \pm 9	746 \pm 9	271 \pm 2	92.8 \pm 0.9	30.6 \pm 0.3	30.6 \pm 0.6	18 \pm 1	16 \pm 9	1.4	...
	model	1146 \pm 31	708 \pm 18	268 \pm 7	94 \pm 3	30.0 \pm 0.8	30.0 \pm 0.8	15.8 \pm 0.4	3.3 \pm 0.1
121504.....	obs	1002 \pm 7	631 \pm 8	225 \pm 1	81.3 \pm 0.8	25 \pm 0.2	27 \pm 2	14 \pm 2	27 \pm 19	1.3	...
	model	976 \pm 35	620 \pm 22	222 \pm 8	79 \pm 3	25 \pm 1	25 \pm 1	13.4 \pm 0.5	2.8 \pm 0.1
141937.....	obs	1393 \pm 10	872 \pm 11	311 \pm 2	110 \pm 1	34.9 \pm 0.3	35.1 \pm 0.5	18 \pm 2	−3 \pm 12	−0.6	...
	model	1365 \pm 38	864 \pm 23	312 \pm 9	111 \pm 3	36 \pm 1	36 \pm 1	18.7 \pm 0.5	4.0 \pm 0.1
179949.....	obs	2943 \pm 21	1849 \pm 23	658 \pm 4	234 \pm 2	73.9 \pm 0.7	71 \pm 1	35 \pm 2	−5 \pm 11	−1.2	1 \pm 10
	model	2822 \pm 78	1809 \pm 49	641 \pm 18	229 \pm 6	73 \pm 2	73 \pm 2	38 \pm 1	8.1 \pm 0.2
190228.....	obs	2068 \pm 15	1283 \pm 16	469 \pm 3	166 \pm 2	52.8 \pm 0.5	53.4 \pm 0.8	29 \pm 3	12 \pm 26	0.2	...
	model	1987 \pm 66	1223 \pm 40	456 \pm 15	164 \pm 5	52 \pm 2	52 \pm 2	27.6 \pm 0.9	5.8 \pm 0.2

NOTES.—Photometry and 1σ internal uncertainties are in units of mJy. Calibration uncertainties are not included in the error estimates. IRS fluxes come from synthetic photometry from IRS low-resolution spectra. Fluxes at 1200 μm are from Carpenter et al. (2005). Rows labeled “model” give the expected stellar contribution from its Kurucz model; those labeled “obs” give the photometric measurement. The S/N of the excess, S/N_{exc}, is the photometric measurement minus the star’s contribution from its Kurucz model divided by the global uncertainty. The global uncertainty is calculated by adding in quadrature the internal and calibration uncertainties, the later taken to be 7% for MIPS 70 μm .

in J. M. Carpenter et al. (2007, in preparation). Infrared excesses can also be identified empirically from the color-color diagrams in Figure 2, showing a narrow distribution of the ratio of the fluxes at 24 and 8 μm (F_{24}/F_8) compared to a wide distribution of the ratio of the fluxes at 70 and 24 μm (F_{70}/F_{24}). This indicates that the flux at 24 μm is mainly photospheric and that the best indicator of the presence of a debris disk is the 70 μm excess emission.

HD 38529 has the only robust detection of an excess at 70 μm with a S/N in the excess emission of 4.7, a small excess at 33 μm (with a S/N in the excess emission of 2.1), and no excess <30 μm . Because of the slope of the spectrum across the MIPS 70 μm band, the 70 μm flux needs to be color corrected by dividing the observed flux by 0.893 (assuming the emission arises from cold dust emitting like a blackbody at 50 K; see the MIPS Data Handbook). This increases the 70 μm flux from 75.3 to 84.3 mJy. The centroid positions of the object in the 24 and 70 μm images are R.A. = 05^h46^m34.88^s, decl. = +01°10′04.61″ and R.A. = 05^h46^m34.79^s, decl. = +01°10′04.62″, respectively, in agreement with the 2004.7 2MASS coordinates for HD 38529 (R.A. = 05^h46^m34.895^s and decl. = +01°10′04.65″, accounting for the proper motion of the star, with the absolute pointing knowledge, better than 1.4″ and 1.7″ (1σ radial) at 24 and 70 μm , respectively (*Spitzer* Observers Manual). Inspection of the images shows that the 24 and 70 μm source is free of nearby point sources, and there is very little structure from galactic cirrus. Finally, it is unlikely that the emission at 70 μm comes from a background galaxy within 2″ of the stellar position; using the background counts in Dole et al. (2004) and following Downes et al. (1986), we estimate a probability of 1.5×10^{-5} for 50 mJy and 7.4×10^{-6} for 100 mJy. We therefore conclude that the observed 70 μm emission comes from HD 38529. Even though it is difficult to identify statistical trends from one detection, it is interesting to note that HD 38529 is the most luminous, most massive, and most evolved of the planet-bearing stars in Table 1. Assuming $V = 5.95$ (Johnson 1966), a *Hipparcos* distance of 42 pc, and no reddening, the object has an

absolute visual magnitude of $M_v = 2.81$ and $\log(L/L_\odot) = 0.82$, putting the star on the Hertzsprung gap, so it is clearly post-main sequence.

In summary, we find that only 1 out of 9 of the planet-bearing stars show evidence of a debris disk. In the next section, we explore whether or not there is evidence of a correlation between the presence of debris disks and close-in planets.

4. ARE DEBRIS DISKS AND CLOSE-IN PLANETS RELATED PHENOMENA?

Using the FEPS data, we address the possibility of a debris-planet connection by comparing the results for the nine planet-bearing stars (hereafter, “the planet sample”) to those of a larger subset of stars in the FEPS sample without regard to the presence of planets (hereafter, “the control sample”). The planet sample is a subset of the control sample. Given the current statistics from RV surveys, it is unlikely that the majority of the stars in the control sample harbor a giant planet; therefore, the control sample is likely less biased for the presence of giant planets than is the planet sample. By comparing these two samples, we investigate whether the frequency and luminosity of debris disks are correlated with the presence of a massive planet.

4.1. Selection of the Control Sample

The main criterion for the choice of the control sample is that the observations reach levels of sensitivity similar to the planet sample. For this we require that (1) the stars in the control sample span the same range of distances as the planet-bearing stars (26–62 pc) and (2) their infrared background levels at 70 μm be similar. Age may also be a factor, as the stars in the FEPS sample typically range from 3 Myr to 3 Gyr, with a few stars perhaps as old as 3–10 Gyr, while planet-bearing stars are typically older than 1 Gyr. If debris disks evolve significantly over the range 3 Myr–10 Gyr, this could also introduce a bias in the debris disk detection. Samples of young stars show an initial rapid decline

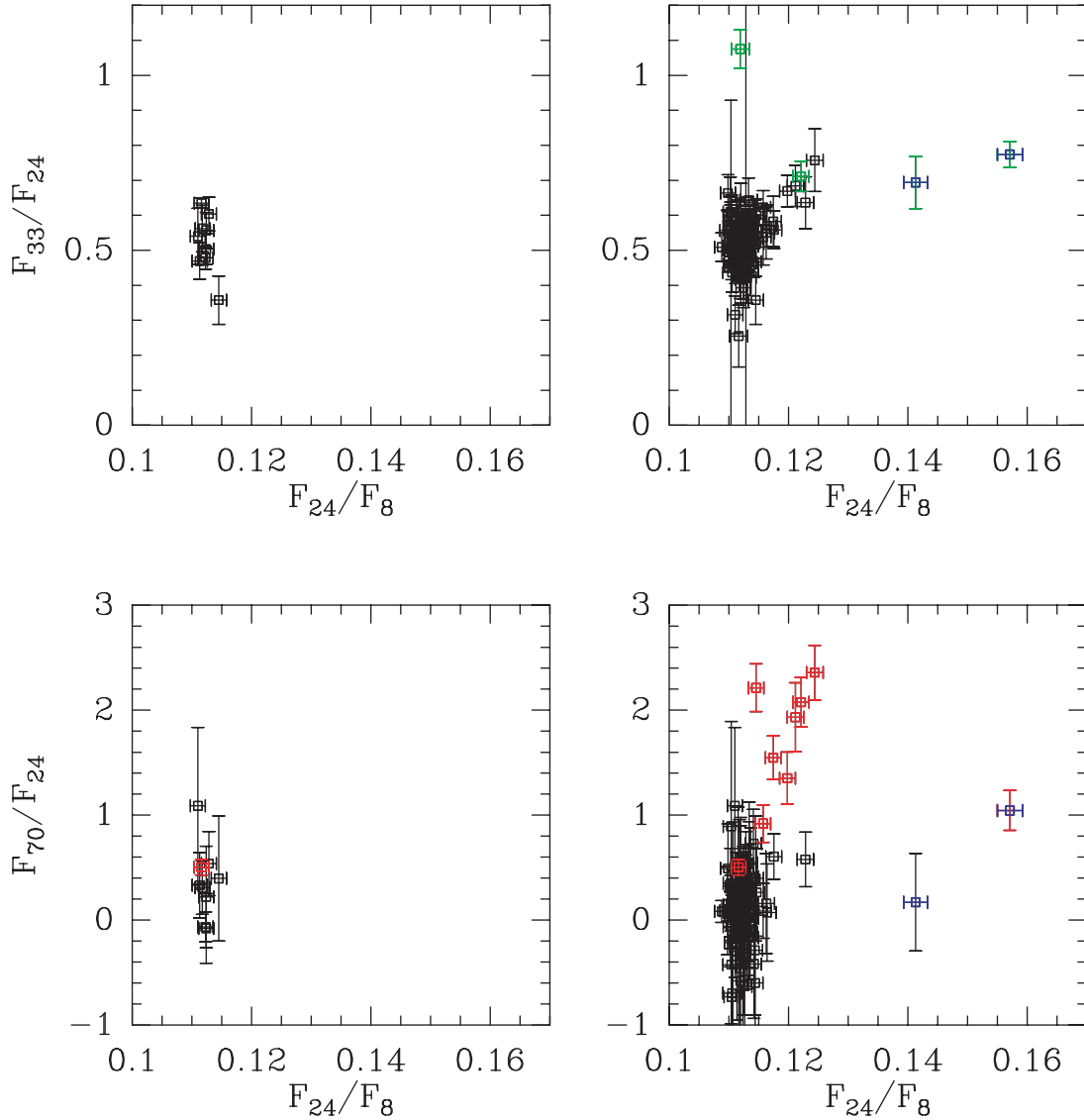


FIG. 2.— Color-color diagrams of the nine stars in the FEPS planet sample (*left*) and the 99 stars in the FEPS control sample (*right*). Stars that show $70\ \mu\text{m}$ excess emission with a S/N in the excess emission >3 are shown in red and include one star in the planet sample (HD 38529) and nine stars in the control sample. Similarly, stars that show 24 and $33\ \mu\text{m}$ excess emission with a S/N in the excess emission >3 are shown in blue and green, respectively, and include only two stars (for $24\ \mu\text{m}$) and four stars (for $33\ \mu\text{m}$) in the control sample and none in the planet sample. [The outlier at (0.114, 0.357) in the upper left panel corresponds to HD 80606; its IRS spectrum is very noisy beyond $30\ \mu\text{m}$, possibly due to a peak-up failure, making the $33\ \mu\text{m}$ point unreliable.]

over the first ~ 100 Myr, while Bryden et al. (2006) found that the excess rate at $70\ \mu\text{m}$ is $13\% \pm 5\%$ (down to a fractional luminosity of $L_{\text{dust}}/L_* \sim 10^{-5}$, i.e., about 100 times the luminosity of the KB dust) and is not correlated with stellar age on Gyr timescales. Therefore, by choosing a control sample that is restricted to stars older than 300 Myr, we do not expect to introduce any significant age bias, while improving the statistics by increasing the number of stars in the control sample. Our control sample thus consists of 99 stars with distances 26–62 pc and ages >300 Myr. We use the Kolmogorov-Smirnov (K-S) test (see, e.g., Press et al. 1993) to assess whether or not the distributions of distances and IR background levels of the planet and the control samples are consistent with having been drawn from the same parent population. The K-S test yields two values, D , a measure of the largest difference between the two cumulative distributions under consideration, and probability ($D > \text{observed}$), an estimate of the significance level of the observed value of D as a disproof of the

null hypothesis that the distributions come from the same parent population; i.e., a very small value of probability($D > \text{observed}$) implies that the distributions are significantly different. Because in this case we find probability($D > \text{observed}$) = 0.6 (for distance) and probability($D > \text{observed}$) = 0.4 (for IR background), we conclude that both samples could have been drawn from the same distribution in terms of distance and IR background levels and therefore can be compared. Note that the K-S test for age yields a much lower probability [probability($D > \text{observed}$) $\sim 10^{-5}$]; i.e., both samples are not likely drawn from the same distribution in terms of age. However, given that the observations indicate that for the ages under consideration (>300 Myr, with approximately half of the stars having ages >1 Gyr) there is no correlation between the $70\ \mu\text{m}$ excess and the stellar age, we do not expect to introduce any significant bias by comparing the two samples (but keep in mind that the validity of the comparison relies on the observed lack of correlation with age).

4.2. Frequency of Debris Disks

With respect to the frequency of debris disks, we find that 1/9 stars in the FEPS planet sample have $70\ \mu\text{m}$ excess emission with a S/N in the excess emission >3 , compared to 9/99 stars in the FEPS control sample; for the Bryden et al. (2006) survey, the rates are 1/11 (planet sample) and 7/69 (control sample). Because the frequency of debris disks (seen at $70\ \mu\text{m}$) in the planet sample and the control sample are similar, we conclude that there is no evidence of the presence of a correlation between the frequency of debris disks and close-in planets (if we were to assume a \sqrt{N} error in the number of stars with excesses, the frequency of debris around a planet-bearing star would be within a factor of 3 of the control sample). At $24\ \mu\text{m}$ (tracing warmer dust), the frequency of debris disks could also be similar in the planet and the control samples, as none of the stars in the FEPS planet sample show excess emission, while 2/99 stars in the FEPS control sample do.

4.3. Fractional Excess Luminosity: Survival Analysis

The planet sample and the control sample are dominated by upper limits; therefore, the K-S test is not sufficient to assess the probability that they could have been drawn from the same parent distribution. To extract the maximum amount of information from the nondetections, it is necessary to use survival analysis methods, which make certain assumptions about the underlying distributions. Using ASURV revision 1.2 (Lavalley et al. 1992), which implements the survival analysis methods of Feigelson & Nelson (1985), we have used the Gehan, logrank, and Peto-Prentice tests to compute the probability that the planet sample and the control sample were drawn from the same parent distribution with respect to the fractional excess luminosity, L_{dust}/L_* .

We use the fractional luminosity of the excess, L_{dust}/L_* , instead of the $70\ \mu\text{m}$ excess flux, to minimize any correlation with distance. Following Bryden et al. (2006), from the $70\ \mu\text{m}$ excess emission one can estimate the fractional luminosity of the excess by assuming a single dust temperature, $T_{\text{dust}} = 52.7\ \text{K}$, corresponding to an emission peak at $70\ \mu\text{m}$. In this case, $L_{\text{dust}}/L_* \sim 10^{-5} (5600/T_*)^3 (F_{70,\text{dust}}/F_{70,*})$, where $F_{70,\text{dust}}$ and $F_{70,*}$ are the dust excess and photospheric flux at $70\ \mu\text{m}$ and T_* is the stellar temperature in kelvins. For nondetections, $F_{70,\text{dust}} = 3\Delta F_{70}$, where ΔF_{70} is the $1\ \sigma$ uncertainty of the observed flux.

The resulting survival analysis probabilities, using $3\ \sigma$ upper limits, are 0.64 (Gehan), 0.86 (logrank), and 0.72 (Peto-Prentice). As discussed in Feigelson & Nelson (1985), the logrank test is more sensitive to differences at low values of the variable under consideration (i.e., near the upper limits), while the Gehan test is more sensitive to differences at the high end (i.e., for the detections). The Peto-Prentice test is preferred when the upper limits dominate and the sizes of the samples to be compared differ (as it is our case). Similarly, we have carried out survival analysis for the sample of 69 FGK main-sequence stars in Bryden et al. (2006). This sample was selected with regard to the expected S/N for stellar photospheres and is not biased for or against known planet-bearing stars. The planet sample consists of 11 stars with known close-in planets, and the control sample includes all 69 stars. With respect to the FEPS targets, these stars are generally closer, and the observations are therefore sensitive to less luminous debris disks (see Fig. 3). In this case, the probabilities that the planet sample and the control sample could have been drawn from the same parent distribution with respect to the fractional excess luminosity are 0.83 (Gehan), 0.86 (logrank), and 0.70 (Peto-Prentice). If we consider the FEPS and Bryden samples together, these probabilities are 0.62, 0.85, and 0.70, respectively. Because all the prob-

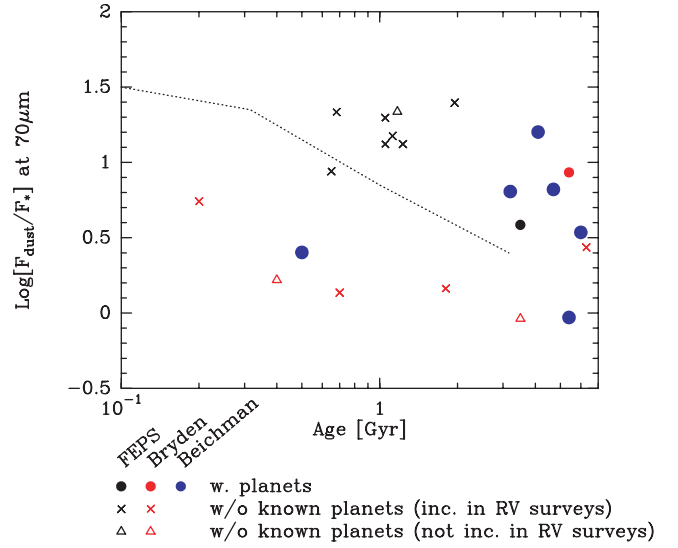


FIG. 3.—Ratio of the excess flux to the photospheric flux for the stars with $70\ \mu\text{m}$ excess emission and a S/N in the excess emission >3 . The shape of the symbol indicates the presence of a close-in planet. Circles represent stars with known RV planets, crosses represent stars without known planets (but included in RV surveys), and triangles represent stars without known planets (not included in RV surveys). The black symbols correspond to stars in the FEPS survey, while blue and red correspond to stars in Beichman et al. (2005) and Bryden et al. (2006), respectively. (The latter includes stars at smaller distances than those in the FEPS sample, so it is sensitive to smaller excesses.) For comparison, the dotted line shows F_{dust}/F_* at $60\ \mu\text{m}$ resulting from the collisional cascade of a planetesimal disk at 30–80 AU (Kenyon & Bromley 2005). Because the collisional physics and the behavior of the debris following the collision are uncertain, the estimate for F_{dust}/F_* at $60\ \mu\text{m}$ could vary by more than a factor of 10, so the observations could be consistent with the model predictions.

abilities are larger than 0.6, i.e., significantly larger than 0, the conclusion from the Gehan, logrank, and Peto-Prentice tests from the data collected so far (from both FEPS and the GTO results in Bryden et al. 2006) is that we cannot rule out the hypothesis that the planet sample and the control sample have been drawn from the same population with respect to the fractional excess luminosity. In other words, we find no sign of correlation between the excess luminosity and the presence of close-in massive planets.

5. DISCUSSION

5.1. Comparison to Previous Studies

Greaves et al. (2004) searched for submillimeter dust emission around eight stars known from RV studies to have giant planets orbiting within a few AU and found no debris disks down to a dust mass limit of $6 \times 10^{-8} M_{\odot}$ ¹⁰; they also noted that out of 20 solar-type stars known to have disks, only one, ϵ Eridani, has a planet orbiting inside a few AU (Hatzes et al. 2000) and concluded that either debris disks and close-in giant planets are unrelated phenomena or they are mutually exclusive. However, these results had severe limitations due to the low sensitivity of the submillimeter observations and the limited accuracy of the RV measurements due to the youth of the sample. The high sensitivity of the mid-IR observations with *Spitzer* allows a fresh reexamination of the question. Preliminary work from a *Spitzer* MIPS GTO program by Beichman et al. (2005) found that out of 26 FGK

¹⁰ Dust mass estimates for the KB dust disk range from a total dust mass $< 3 \times 10^{-10} M_{\odot}$ (Backman et al. 1995) to $\sim 4 \times 10^{-11} M_{\odot}$ for dust particles $< 150\ \mu\text{m}$ (Moro-Martín & Malhotra 2003); with a fractional luminosity of $L_{\text{dust}}/L_* \sim 10^{-7} - 10^{-6}$ (Stern 1996). The fractional luminosity of the asteroid belt dust (namely, zodiacal cloud) is estimated to be $L_{\text{dust}}/L_* \sim 10^{-8}$ to 10^{-7} (Dermott et al. 2002).

field stars known to have planets through RV studies, six stars (HD 33636, HD 50554, HD 52265, HD 82943, HD 117176, and HD 128311) show 70 μm excess with a S/N in excess of 12.4, 12.1, 3.2, 15.7, 3.2 and 4.6, respectively, implying the presence of cool dust (<100 K) located mainly beyond 10 AU. These six stars have a median age of 4 Gyr, and their fractional luminosities, $L_{\text{dust}}/L_{\text{star}}$, in the range $(0.1-1.2) \times 10^{-4}$ are ~ 100 times that inferred for the KB (Beichman et al. 2005). The study suggested a tentative correlation between the frequency and magnitude of the dust emission with the presence of known planets. Our analysis of the FEPS and the Bryden et al. (2006) samples does not confirm the presence of such a correlation.

5.2. Interpretation of Our Results

We found that, given the *Spitzer* and RV data we have so far, there is no evidence of a correlation between the presence of close-in massive planets and the frequency and excess luminosity of debris disks; i.e., debris disks are not more prevalent in systems with close-in massive planets than in systems selected without regard to whether they have close-in massive planets or not. This might seem a surprising result, because it is reasonable to assume that most giant planets formed in systems that were initially rich in planetesimals, as planetesimals are the building blocks of giant planets in the core-accretion model. However, despite a likely initial abundance of dust-producing planetesimals, systems with giant planets may not produce abundant debris at Gyr ages. The solar system is one example in which there is significant evidence that it once had a massive planetesimal belt despite the little debris produced today. That is, giant planets may play an important role in the evolution of debris disks by efficiently grinding away or ejecting planetesimals from an initially massive disk. This could involve processes similar to the LHB in the early solar system, where a large fraction of the dust-producing planetesimals were lost due to the orbital migration of the giant planets. For the planet-bearing stars, if the conditions for the formation of at least one giant planet were met, we could speculate that additional massive planets possibly formed and migrated, which could lead to LHB-type events. Comparison of the debris disk properties between stars with and without massive giant planets may therefore be a function of age. The FEPS and Bryden et al. (2006) samples are drawn mainly from stars 300 Myr to 10 Gyr old, i.e., mostly after the LHB is thought to have occurred in our solar system.

Our result also suggests that massive planets may not be required to produce debris. A possible mechanism for the production of debris in the presence or absence of massive planets is the collisional cascade model of Kenyon & Bromley (2005). Such a model can produce debris at Gyr ages, even in disks that are too low in solids to form a giant planet (i.e., too low in initial disk mass and/or too low in metallicity). In this model, large (1000 km) planetesimals can stir up smaller planetesimals (0.1–10 km in size) along their orbits, starting a collisional cascade that can produce dust excess emission of the magnitude shown in Figure 3 over the relevant range of ages. However, this cannot be the only mechanism, because if it were to dominate debris production, one would expect to see the dust temperature correlated with age, but this trend has not been observed (Najita & Williams 2005). Similarly, the observations in Figure 3 could not confirm the time dependence of the fractional 70 μm excess emission predicted by the models.

That massive planets may not be required to produce debris is also supported by several observational results. First, debris disks are more common than massive planets. It is found that $>7\%$ of stars have giant planets with $M < 13 M_J$ and semimajor axis within 5 AU, but this is a lower limit, because the duration of the surveys (6–8 yr) limits the ability to detect planets between 3 and

5 AU. The expected frequency of gas giant planets increases to $\sim 12\%$ when RV surveys are extrapolated to 20 AU (Marcy et al. 2005), with the distribution of planets following $dN/dM \propto M^{-1.05}$ from 1 M_S to 10 M_J (where the subscripts S and J refer to Saturn and Jupiter, respectively; the surveys are incomplete at smaller masses). In comparison, the frequency of debris disks observed at 70 μm with *Spitzer* is $13\% \pm 5\%$ (from Bryden et al. 2006). However, this detection rate is sensitivity limited, because the observations in Bryden et al. (2006) can only reach fractional luminosities of $L_{\text{dust}}/L_* \gtrsim 10^{-5}$, i.e., $\gtrsim 100$ times the luminosity from our solar system KB. Bryden et al. (2006) found that the frequency of dust detection increases steeply as smaller fractional luminosities are considered, ranging from nearly 0% for $L_{\text{dust}}/L_* \sim 10^{-3}$ to $2\% \pm 2\%$ for $L_{\text{dust}}/L_* \sim 10^{-4}$ and $13\% \pm 5\%$ for $L_{\text{dust}}/L_* \sim 10^{-5}$. Using this cumulative distribution and assuming that the distribution of debris disk luminosities is a Gaussian, Bryden et al. (2006) estimated that the luminosity of the solar system dust is consistent with being 10 times brighter or fainter than an average solar-type star; i.e., debris disks at the solar system level could be common. The debris disks observed with *Spitzer* could therefore be the high-luminosity tail of a distribution of dust luminosities that peaks near the solar system values.

Second, there is no correlation between stellar metallicities and the incidence of debris disks (Beichman et al. 2005; Bryden et al. 2006; Greaves et al. 2006). Greaves et al. (2006) found that in a sample of 310 F7–K3 stars within 25 pc of the Sun and for which the stellar metallicities are known, there is only a 0.6% probability that planet-bearing stars and debris disks stars have the same metallicity distribution, with the planet-bearing stars being correlated with high stellar metallicities (Fischer & Valenti 2005). This is in agreement with the core-accretion model, in which the formation of giant planets requires the presence of a large surface density of solids in the disk, so that the planet can grow a core sufficiently large to accrete an atmosphere before the gas disk disappears in $\lesssim 10$ Myr. Because the governing time-scale in the growth of planetesimals is the orbital period, in the KB region the planetesimal formation process is slower (according to Kenyon & Bromley [2004], it may take ~ 3 Gyr to form a Pluto at 100 AU), but can proceed well after the gas disk has dissipated (so there is no time limitation). This can occur in systems regardless of whether or not they meet the conditions for giant planet formation.

As a result, collisional grinding in a self-stirred model of this kind might be expected to produce debris in systems with low metallicities and low initial disk masses. If this leads to debris production in a wider variety of systems than can produce giant planets, we might expect the presence of debris to be poorly correlated with the presence of giant planets.

6. CONCLUSIONS

1. Using *Spitzer* observations, we have searched for debris disks around nine planet-bearing solar-type stars, with stellar ages ranging from 2 to 10 Gyr. Only one of the sources, HD 38529, is found to have excess emission above the stellar photosphere, with a S/N at 70 μm of 4.7 and no excess at $\lambda < 30 \mu\text{m}$. The remaining sources show no excesses at any *Spitzer* wavelengths.

2. Given the data we have so far, from both FEPS and the FGK sample from Bryden et al. (2006) and using survival analysis, we find that there is no evidence of a correlation between the presence of close-in massive planets and the frequency and excess luminosity of debris disks.

3. Because we expect massive planets to form in systems that are initially rich in planetesimals, but the observations indicate that systems with giant planets do not preferentially show debris,

there is the possibility that massive planets play an important role in the evolution of debris disks by efficiently grinding away or ejecting planetesimals from an initially massive disk, possibly in a LHB-type event.

4. Our results also suggest that massive planets may not be required to produced debris, which is supported by the collisional cascade models of Kenyon & Bromley (2005) and the observations and theoretical models that indicate that debris disks are more prevalent than massive planets.

We thank the rest of the FEPS team members, colleagues at the *Spitzer* Science Center (in particular, Dave Frayer), and members of all the *Spitzer* instrument teams for advice and support. We

thank G. Marcy, R. P. Butler, S. S. Vogt, and D. A. Fischer for their work with Keck HIRES and the anonymous referee for useful comments. This work is based on observations made with the *Spitzer* Space Telescope, which is operated by the Jet Propulsion Laboratory (JPL), California Institute of Technology, under NASA contract 1407. A. M.-M. is under a contract with JPL funded by NASA through the Michelson Fellowship Program. A. M.-M. is also supported by the Lyman Spitzer Fellowship at Princeton University. M. R. M. and R. M. are supported in part through the LAPLACE node of the NASA Astrobiology Institute. R. M. also acknowledges support from the NASA Origins of Solar Systems research program. S. W. was supported through the DFG Emmy Noether grant WO 875/2-1 and WO875/2-2. FEPS is pleased to acknowledge support from NASA contracts 1224768 and 1224566 administered through JPL.

APPENDIX

HD 150706

HD 150706 is a member of of the FEPS sample and exhibits an excess emission at $70\ \mu\text{m}$ with a S/N in the excess emission of 4.3 (and a color-corrected flux of 46.3 mJy). Even though it has been listed as a planet-bearing star, it is not included in our planet sample, because new RV observations cannot confirm the claimed planet. HD 150706 has appeared in various compilations of Sun-like stars with extrasolar planets (cf. Santos et al. 2004). An orbital solution for a purported $1.0\ M_J$ eccentric planet at 0.8 AU was announced by the Geneva Extrasolar Planet Search Team (the 2002 Washington conference of Scientific Frontiers in Research in Extrasolar Planets; Udry et al. 2003); however, there is no refereed discovery paper giving details, only Web pages. Eight Doppler velocity measurements (Table 4) made with HIRES on the Keck telescope from 2002 to 2006 yield rms values of $12.1\ \text{m s}^{-1}$, far below the $33\ \text{m s}^{-1}$ velocity amplitude claimed due to a planet. The rms for a linear fit of the HIRES data is $8\ \text{m s}^{-1}$, which can be adequately explained by the expected jitter for a young ($700 \pm 300\ \text{Myr}$), active early G star such as HD 150706. The four years of HIRES data rule out the presence of planets of roughly $1\ M_J$ or larger located within 2 AU and $2\ M_J$ or more within 5 AU (modulo $\sin i$). Smaller planets inward of 5 AU and super-Jupiters outward of 5 AU are not inconsistent with the HIRES observations to date. Further, the lack of a monotonic trend in the velocities of amplitude many tens of m s^{-1} indicates that there is no brown dwarf or low-mass star anywhere within $\sim 20\ \text{AU}$.

TABLE 4
RELATIVE RADIAL VELOCITIES FOR HD 150706

Julian Date (−2,450,000)	Radial Velocity (m s^{-1})
2,514.728.....	-0.40 ± 1.8
2,538.717.....	-3.59 ± 1.9
2,713.091.....	4.20 ± 1.7
2,806.008.....	-9.49 ± 2.0
2,850.896.....	-5.08 ± 1.8
3,179.924.....	0.00 ± 1.7
3,427.128.....	23.83 ± 2.2
3,842.061.....	20.89 ± 2.2

REFERENCES

- Aumann, H. H., et al. 1984, *ApJ*, 278, L23
Backman, D. E., Dasgupta, A., & Stencel, R. E. 1995, *ApJ*, 450, L35
Backman, D. E., & Paresce, F. 1993, in *Protostars and Planets III*, ed. E. H. Levy & J. I. Lunine (Tucson: Univ. Arizona Press), 1253
Barbieri, M., & Gratton, R. G. 2002, *A&A*, 384, 879
Beichman, C. A., et al. 2005, *ApJ*, 622, 1160
Bernstein, G. M., Trilling, D. E., Allen, R. L., Brown, M. E., Holman, M., & Malhotra, R. 2004, *AJ*, 128, 1364
Bryden, G., et al. 2006, *ApJ*, 636, 1098
Butler, R. P., et al. 2006, *ApJ*, 646, 505
Cannon, A. J., & Pickering, E. C. 1918–1924, *The Henry Draper Catalogue* (Cambridge: The Observatory)
Carpenter, J. M., Wolf, S., Schreyer, K., Launhardt, R., & Henning, T. 2005, *AJ*, 129, 1049
Dermott, S. F., Kehoe, T. J. J., Durda, D. D., Grogan, K., & Nesvorný, D. 2002, in *Proc. Asteroids, Comets, Meteors*, ed. B. Warmbein (ESA SP-500; Noordwijk: ESA), 319
Dole, H., et al. 2004, *ApJS*, 154, 87
Downes, A. J. B., Peacock, J. A., Savage, A., & Carrie, D. R. 1986, *MNRAS*, 218, 31
Fazio, G. G., et al. 2004, *ApJS*, 154, 10
Feigelson, E. D., & Nelson, P. U. 1985, *ApJ*, 293, 192
Fischer, D. A., & Valenti, J. A. 2005, *ApJ*, 622, 1102
Gomes, R., Levison, H. F., Tsiganis K., & Morbidelli, A. 2005, *Nature*, 435, 466
Gonzalez, G., Laws, C., Tyagi, S., & Reddy, B. E. 2001, *AJ*, 121, 432
Gorlova, N., et al. 2006, *ApJS*, 154, 448
Greaves, J. S., Fischer, D. A., & Wyatt, M. C. 2006, *MNRAS*, 366, 283
Greaves, J. S., Holland, W. S., Jayawardhana, R., Wyatt, M. C., & Dent, W. R. F. 2004, *MNRAS*, 348, 1097
Hatzes, A. P., et al. 2000, *ApJ*, 544, L145
Hines, D. H., et al. 2005, *FEPS Data Explanatory Supplement*, Version 2.1 (Pasadena: SSC)
Houck, J. R., et al. 2004, *ApJS*, 154, 18
Houk, N. 1980, *Michigan Catalog of HD Stars*, Vol. 3 (Ann Arbor: Univ. Michigan Press)

- Houk, N., & Cowley, A. P. 1975, *Michigan Catalog of HD Stars*, Vol. 1 (Ann Arbor: Univ. Michigan Press)
- Houk, N., & Smith-Moore, M. 1988, *Michigan Catalog of Two-Dimensional Spectral Types for the HD Stars*, Vol. 4 (Ann Arbor: Univ. Michigan Press)
- Houk, N., & Swift, C. 1999, *Michigan Catalog of Two-Dimensional Spectral Types for the HD Stars*, Vol. 5 (Ann Arbor: Univ. Michigan Press)
- Ibukiyama, A., & Arimoto, N. 2002, *A&A*, 394, 927
- Jaschek, M. 1978, *Bull. Inf. Cent. Donnees Stellaires*, 15, 121
- Johnson, H. L., Iriarte, B., Mitchell, R. L., & Wisniewskij, W. Z. 1966, *Comm. Lunar. Planet. Lab.*, 4, 99
- Kenyon, S. J., & Bromley, B. C. 2004, *AJ*, 127, 513
- . 2005, *AJ*, 130, 269
- Kim, J. S., et al. 2005, *ApJ*, 632, 659
- Lavalley, M., Isobe, T., & Feigelson, E. 1992, in *ASP Conf. Ser. 25, Astronomical Data Analysis Software and Systems I*, ed. D. M. Worrall, C. Biemesderfer, & J. Barnes (San Francisco: ASP), 245
- Laws, C., Gonzalez, G., Walker, K. M., Tyagi, S., Dodsworth, J., Snider, K., & Suntzeff, N. B. 2003, *ApJ*, 125, 2664
- Levison, H. F., Morbidelli, A., Gomes, R., & Backman, D. 2007, in *Protostars and Planets V*, ed. B. Reipurth, D. Jewitt, & K. Keil (Tucson: Univ. Arizona Press), 951
- Liou, J. C., & Zook, H. A. 1999, *AJ*, 118, 580
- Luu, J. X., & Jewitt, D. C. 2002, *ARA&A*, 40, 63
- Makovoz, D., & Marleau, F. R. 2005, *PASP*, 117, 1113
- Malhotra, R., Duncan, M. J., & Levison, H. F. 2000, in *Protostars and Planets IV*, ed. V. Mannings, A. P. Boss, S. S. Russell (Tucson: Univ. Arizona), 1231
- Marcy, G., Butler, R. P., Fischer, D., Vogt, S., Wright, J. T., Tinney, C. G., & Jones, H. R. A. 2005, *Prog. Theor. Phys. Suppl.*, 158, 24
- Mayor, M., Udry, S., Naef, D., Pepe, F., Queloz, D., Santos, N. C., & Burnet, M. 2004, *A&A*, 415, 391
- Meyer, M. R., Backman, D. E., Weinberger, A. J., & Wyatt, M. C. 2007, in *Protostars and Planets V*, ed. B. Reipurth, D. Jewitt, & K. Keil (Tucson: Univ. Arizona Press), 573
- Meyer, M. R., Hillenbrand, L. A., Backman, D. E., Beckwith, S., Bouwman, J., et al. 2006, *PASP*, 118, 1690
- Meyer, M. R., et al. 2004, *ApJS*, 154, 42
- Moro-Martín, A., & Malhotra, R. 2002, *AJ*, 124, 2305
- . 2003, *AJ*, 125, 2255
- . 2005, *ApJ*, 633, 1150
- Moro-Martín, A., & Malhotra, R., Carpenter, J. M., Hillenbrand, L. A., & Wolf, S. 2007, *ApJ*, submitted
- Naef, D., et al. 2001, *A&A*, 375, L27
- Najita, J., & Williams, J. P. 2005, *ApJ*, 635, 625
- Nordstrom, B., et al. 2004, *A&A*, 418, 989
- Perrier, C., Sivan, J.-P., Naef, D., Beuzit, J. L., Mayor, M., Queloz, D., & Udry, S. 2003, *A&A*, 410, 1039
- Perryman, M. A. C., et al. 1997, *A&A*, 323, L49
- Press, W. H., Flannery, B. P., Teukolsky, S. A., & Vetterling, W. T. 1993, *Numerical Recipes in FORTRAN 77* (Cambridge: Cambridge Univ. Press)
- Reach, W. T., et al. 2005, *PASP*, 117, 978
- Rieke, G. H., et al. 2004, *ApJS*, 154, 25
- . 2005, *ApJ*, 620, 1010
- Santos, N. C., Israelian, G., & Mayor, M. 2004, *A&A*, 415, 1153
- Siegler, N., Muzerolle, J., Young, E. T., Rieke, G. H., Mamajek, E., Trilling, D. E., Gorlova, N., & Su, K. Y. L. 2007, *ApJ*, 654, 580
- Stauffer, J. R., et al. 2005, *AJ*, 130, 1834
- Stern, S. A. 1996, *AJ*, 112, 1203
- Strom, R. G., Malhotra, R., Ito, T., Yoshida, F., & Kring, D. A. 2005, *Science*, 309, 1847
- Udry, S., Mayor, M., Naef, D., Pepe, F., Queloz, D., Santos, N. C., & Burnet, M. 2002, *A&A*, 390, 267
- Udry, S., Mayor, M., & Queloz, D. 2003, in *ASP Conf. Ser. 294, Scientific Frontiers in Research on Extrasolar Planets*, ed. D. Deming & S. Seager (San Francisco: ASP), 17
- Valenti, J. A., & Fischer, D. A. 2005, *ApJS*, 159, 141
- Wright, J. T., Marcy, G. W., Butler, R. P., & Vogt, S. S. 2004, *ApJS*, 152, 261